Active induction balance method for metal detector sensing head utilizing transmitter-bucking and dual current source

2013 J. Phys.: Conf. Ser. 450 012047

(http://iopscience.iop.org/1742-6596/450/1/012047)

Active induction balance method for metal detector sensing head utilizing transmitter-bucking and dual current source

D Ambruš, D Vasić and V Bilas

University of Zagreb, Faculty of Electrical Engineering and Computing
FER-ZESOI, Unska 3, HR-10000 Zagreb, Croatia

E-mail: davorin.ambrus@fer.hr, darko.vasic@fer.hr, vedran.bilas@fer.hr

Abstract. A central problem in a design of frequency domain electromagnetic induction sensors used in landmine detection is an effective suppression of a direct inductive coupling between the transmitter and the receiver coil (induction balance, IB). In sensing heads based on the transmitter-bucking configuration, IB is achieved by using two concentric transmitter coils with opposing exciter fields in order to create a central magnetic cavity for the receiver coil. This design has numerous advantages over other IB methods in terms of detection sensitivity, spatial resolution, sensor dimensions and suitability for model-based measurements. However, very careful design and precise sensing head geometry are required if a single excitation source is used for driving both transmitter coils. In this paper we analyze the IB sensitivity to small perturbations of geometrical properties of coils. We propose a sensor design with dual current source and active induction balance scheme which overcomes the limitations of geometry-based balancing and potentially provides more efficient compensation of soil effects.

1. Introduction

Electromagnetic induction (EMI) sensors have been used for the detection of metallic parts of landmines since the World War II and are nowadays considered a rather mature technology [1]. However, in spite of recent developments in other landmine detection techniques, EMI sensors still remain an area of active research, [2]. Due to their sensitivity, robustness and high-speed operation, they are practically the only sensors that are currently used in humanitarian demining for close-in detection in the field [1], [2].

Time-domain (TD) or pulse induction (PI) EMI sensors transmit a primary magnetic field of pulse waveform and detect a weak secondary field induced by eddy-currents in the metallic object after the transmitter has been shut-off. Since the receiver responses corresponding to the primary and the secondary field are separated in time, TD sensors are inherently balanced which greatly simplifies sensor design. However, their fundamental limitation is the available excitation spectrum band (i.e. the equivalent time frames that eventually cannot capture ‘very early’ or ‘very late’ time data) [2].

Frequency-domain (FD) EMI sensors provide better control over the power and frequency content of the excitation spectrum. Also, they generally claim higher sensitivity and improved SNR (signal-to-noise) response in metal detector applications when compared to TD sensors [2]. On the other hand, in order to explore their benefits an efficient method of primary field suppression (induction balance, IB) must be provided. There are several IB methods that are normally used for design of FD EMI sensors: physical separation of transmit (TX) and receive (RX) coils [3], RX coils in gradiometer configuration, overlapping TX and RX coils (OO and DD types) [4], orthogonal coil arrangement, etc.

All of the above IB implementations have some apparent drawbacks when it comes to design of sensing head for a handheld landmine detector with additional model-based metal characterization features. Such sensor needs to have simple and compact geometry, high detection sensitivity, high spatial resolution and pinpointing accuracy. It also must provide good invertibility of the measured data so that the parameters of a model can be reliably computed. Based on these requirements, a sensing head configuration based on the transmitter-bucking approach is proposed [3].

2. Sensing head design

The initial parameter for the design of a landmine detector sensing head is the diameter of its main transmitter coil D_1 which can be used as a rough estimate of the sensor's maximum ground penetration depth [2]. Having in mind the practical requirements of landmine detection, we set D_1 at 30 cm. Other geometrical properties of the sensing head (coil diameters and number of turns) are obtained from D_1 and the given mathematical model of the chosen coil configuration.

2.1. Transmitter-bucking configuration

The transmitter stage consists of two concentric coplanar coils (TX1 and TX2) driven by AC current of opposite direction so as to create a central region in which the receiver coil senses zero primary field, figure 1. If a circular current loop approximation is used for both TX1 and TX2 coils, the expression for vertical component of magnetic field B_Z as a function of radial distance r from the coil centre and observed at a plane coplanar with the sensing head (i.e. at z=0) can be written as [3]:

$$B_Z(r) = \frac{\mu_0 IN}{2R}\left[1 + \sum_{n=1}^{\infty}\left[\frac{(2n-1)!!}{(2n)!!}\right]^2 (2n+1)\left(\frac{r}{R}\right)^{2n}\right] \qquad \text{for } r \le R, \text{ inside loop} \qquad (2.1)$$

$$B_Z(r) = -\frac{\mu_0 IN}{2R}\left[\frac{1}{2}\left(\frac{R}{r}\right)^2 + \sum_{n=1}^{\infty}\left[\frac{(2n+1)!!}{(2n+2)!!}\right]^2 (2n+2)\left(\frac{R}{r}\right)^{2n+2}\right] \qquad \text{for } r \ge R, \text{ outside loop} \qquad (2.2)$$

I is the transmitter coil current, μ_0 is the magnetic permeability of vacuum (μ_r=1 for free space), N is the number of turns and R is the radius of the transmitter coil. The expressions are obtained by differentiating the Taylor series representation of magnetic scalar potential and assuming azymuthal symmetry [2]. The voltage induced in the RX coil is proportional to the magnetic flux, i.e. the surface integral of magnetic field components from TX1 coil (B_z^1) and TX2 coil (B_z^2) over the circular area defined by the receiver coil radius r, figure 2. The magnetic cavity is created under condition (2.3).

$$\int_0^r B_Z^1(r)\, 2\pi r dr = \int_0^r B_Z^2(r)\, 2\pi r dr \qquad (2.3)$$

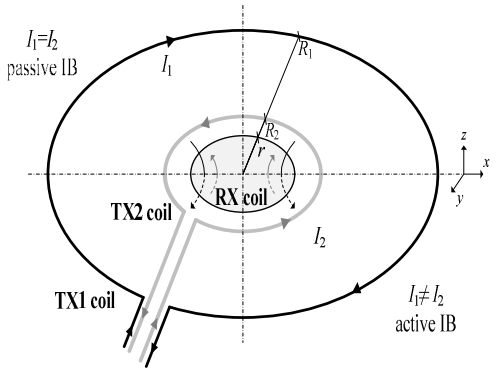

Figure 1. Block diagram of the sensing head in transmitter-bucking configuration.

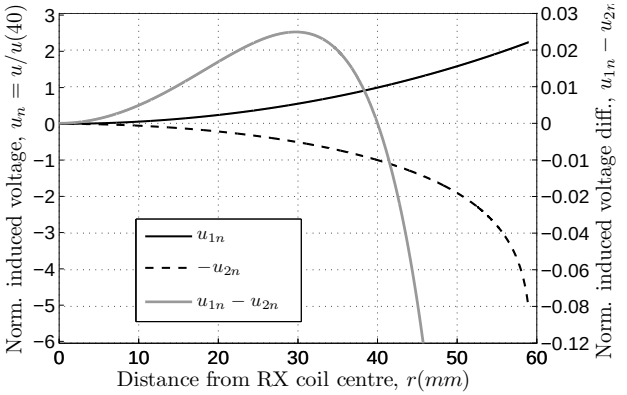

Figure 2. Normalized voltages induced in RX coil in response to TX1 and TX2 coils. IB is obtained for RX coil with radius r=40 mm.

Substituting (2.1) into (2.3) for TX1 and TX2 coils yields an expression (2.4), which describes the mutual dependence of all geometrical parameters of a sensing head (coils radii and number of turns).

$$\frac{N_1}{R_1}\sum_{n=0}^{\infty}\left[\frac{(2n-1)!!}{(2n)!!}\right]^2\frac{(2n+1)}{(2n+2)}\left(\frac{r}{R_1}\right)^{2n}=\frac{N_2}{R_2}\sum_{n=0}^{\infty}\left[\frac{(2n-1)!!}{(2n)!!}\right]^2\frac{(2n+1)}{(2n+2)}\left(\frac{r}{R_2}\right)^{2n} \tag{2.4}$$

Based on (2.4) and initially selected sensing head size, we set the following coil parameters: R_1=15cm, N_1=12 (TX1 coil), R_2=6cm, N_2=4 (TX2 coil) and r =4cm (RX coil).

2.2. Induction balance sensitivity analysis.

In order to analyze the influence of small variations of coil's geometrical parameters on sensor balancing, we define the induction balance sensitivity S_x^u to the parameter x, (2.5)-(2.7).

$$\frac{\Delta u}{u_{IB}}=\frac{\Delta u_1}{u_1}-\frac{\Delta u_2}{u_2} \tag{2.5}$$

$$u_{IB}(r,R,N)=u_1(r,R_1,N_1)=u_2(r,R_2,N_2)=\frac{kN_1}{R}r^2\sum_{n=0}^{\infty}\left[\frac{(2n-1)!!}{(2n)!!}\right]^2\frac{(2n+1)}{(2n+2)}\left(\frac{r}{R}\right)^{2n} \tag{2.6}$$

$$S_x^u=\frac{\Delta u}{u_{IB}}\left(\frac{\Delta x}{x}\right)^{-1}=\left(\frac{\Delta u_1}{u_1}-\frac{\Delta u_2}{u_2}\right)\left(\frac{\Delta x}{x}\right)^{-1}=S_x^{u_1}-S_x^{u_2} \tag{2.7}$$

In (2.5)-(2.7), u_1 and u_2 are voltages induced by TX1 and TX2 coils (respectively), u is the total voltage induced in RX coil by both TX1 and TX2 coils (u_1-u_2), u_{IB} is the voltage induced by a single transmitter coil for a balanced sensor, and k is the coefficient dependent on transmitter current, frequency and RX coil properties. From (2.7), IB sensitivity can be calculated as a difference of equivalent sensitivities of voltages induced by TX1 coil ($S_x^{u_1}$) and TX2 coil ($S_x^{u_1}$), respectively.

The induction balance sensitivity to small variations of TX1 coil radius R_1 can be found by differentiating the expression for $u_1(R_1)$, (2.6), yielding equivalent sensitivity of u_1, (2.8).

$$S_{R_1}^{u_1}=\frac{\partial u_1}{\partial R_1}\frac{R_1}{u_1}=-1-\frac{1}{u_1}\frac{kN}{R_1}r^2\sum_{n=0}^{\infty}\left[\frac{(2n-1)!!}{(2n)!!}\right]^2\frac{(2n+1)}{(2n+2)}2n\left(\frac{r}{R_1}\right)^{2n} \tag{2.8}$$

As expected, the obtained sensitivity to ΔR_1 is nonlinear and contains the expression part that is almost identical to u_1, except for the *2n* term that multiplies each component of the series. Rewriting the Taylor series components in form of two vectors of length *m+1* ($\boldsymbol{u_1}$ and $\boldsymbol{w}$) and neglecting the higher-order terms (under the assumption of the Taylor series sum convergence), (2.9)-(2-10), we obtain the approximate expression for $S_{R_1}^{u_1}$, (2.11). Since $S_{R_1}^{u_2}=0$, IB sensitivity $S_{R_1}^{u}$ is equal to $S_{R_1}^{u_1}$.

$$\boldsymbol{u_1}=\left[0\quad\cdots\quad\left(\frac{(2m-1)!!}{(2m)!!}\right)^2\frac{(2m+1)}{(2m+2)}\left(\frac{r}{R_1}\right)^{2m}\right] \tag{2.9}$$

$\boldsymbol{w}=[0\quad 2\quad 4\quad\cdots\quad 2m]$, $\boldsymbol{i}$ - the unit vector of length *m+1* (2.10)

$$S_{R_1}^{u}=S_{R_1}^{u_1}-S_{R_1}^{u_2}\approx-\left(1+\frac{\boldsymbol{u_1}\cdot\boldsymbol{w}}{\boldsymbol{u_1}\cdot\boldsymbol{i}}\right)-0=-\left(1+\frac{\boldsymbol{u_1}\cdot\boldsymbol{w}}{\boldsymbol{u_1}\cdot\boldsymbol{i}}\right) \tag{2.11}$$

It can be easily shown that the same analysis applies to the case of IB sensitivity to small variations of TX2 coil radius R_2. If R_1 is substituted with R_2 in (2.8) and (2.9), and the corresponding vector notation $\boldsymbol{u_2}$ is introduced, the approximate expression for the IB sensitivity $S_{R_2}^{u}$ is given by (2.12).

$$S_{R_2}^{u}=S_{R_2}^{u_1}-S_{R_2}^{u_2}\approx 0-(-1)\left(1+\frac{\boldsymbol{u_2}\cdot\boldsymbol{w}}{\boldsymbol{u_2}\cdot\boldsymbol{i}}\right)=1+\frac{\boldsymbol{u_2}\cdot\boldsymbol{w}}{\boldsymbol{u_2}\cdot\boldsymbol{i}} \tag{2.12}$$

The above procedure can also be applied to the calculation of IB sensitivity to small variations of RX coil radius r. By differentiating $u_1(r)$ and $u_2(r)$, and calculating equivalent voltage sensitivities as in (2.8)-(2.11), an expression for S_r^u can be derived. In (2.13), $\boldsymbol{w}$ = [0 2 4···(2m+2)], length $m+1$.

$$S_r^u = S_r^{u_1} - S_r^{u_2} \approx \frac{\boldsymbol{u_1 \cdot w}}{\boldsymbol{u_1 \cdot i}} - \frac{\boldsymbol{u_2 \cdot w}}{\boldsymbol{u_2 \cdot i}} \tag{2.13}$$

Finally, IB sensitivity to x may also be expressed in absolute terms, (2.14). The voltage imbalance Δu additionally depends on the number of turns of RX coil N_r and the operating frequency ω.

$$\Delta u = S_x^u \frac{\Delta x}{x} u_{IB}, \qquad u_{IB} \sim N_r \omega \tag{2.14}$$

3. Active induction balance technique

The induction balance method analyzed so far is of passive type, based only on geometrical properties of the transmitter-bucking coil configuration, (2.4). By that, it is assumed that TX coils are fed with the excitation current of the same amplitude and of opposite phase. If TX1 and TX2 coil currents are controlled separately (I_1 and I_2), an active IB scheme is achievable under the condition (3.1).

$$\frac{I_1 N_1}{R_1} \sum_{n=0}^{\infty} \left[\frac{(2n-1)!!}{(2n)!!} \right]^2 \frac{(2n+1)}{(2n+2)} \left(\frac{r}{R_1} \right)^{2n} = \frac{I_2 N_2}{R_2} \sum_{n=0}^{\infty} \left[\frac{(2n-1)!!}{(2n)!!} \right]^2 \frac{(2n+1)}{(2n+2)} \left(\frac{r}{R_2} \right)^{2n} \tag{3.1}$$

3.1. Effects of active induction balance

In order to investigate the effectiveness of the active induction balance (AIB) approach, a simple sensitivity analysis is performed. The corresponding sensitivities of voltages induced in the receiver coil to small perturbations of I_1 and I_2 can be easily calculated from (3.1), based on considerations given in chapter 2.2, yielding (3.2) and (3.3).

$$S_{I_1}^u = S_{I_1}^{u_1} - S_{I_1}^{u_2} = 1 - 0 = 1 \tag{3.2}$$

$$S_{I_2}^u = S_{I_2}^{u_1} - S_{I_2}^{u_2} = 0 - 1 = -1 \tag{3.3}$$

From the above expressions, it is evident that the obtained sensitivities are linear and that small sensor imbalances caused by geometry imperfections or by coils of finite length can be effectively compensated by applying a correction signal to either I_1or I_2, i.e. ΔI. In principle, it is better to use I_2 as a balancing source so that the far field distribution of the main transmitter (i.e. coil with a higher magnetic moment, TX1) remains virtually unaffected.

Another important advantage of the AIB approach is that a dynamic IB method can be introduced to automatically compensate for imbalances caused by the effects of non-cooperative (mainly magnetic) soils. Although the transmitter-bucking configuration is clearly not the best choice when it comes to sensing head sensitivity to soil effects [4], other coil configurations lack the practical opportunity to implement AIB. Sensors with passive IB generally cope with the soil problem on the receiver side, by appropriate signal processing techniques. However, these methods usually suffer from the reduction of dynamic range and sensitivity of metal detection [2].

3.2. Current source design

Proper design of the excitation source circuit is crucial for the implementation of AIB technique. For a landmine detector application, a current source is a preferred solution over a voltage source. In the former case, the magnitude of the excitation current (and thus the transmitted magnetic field) is kept constant and basically unaffected by the coil impedance, soil properties, as well as the lift-off and orientation of the sensing head (when the sensor is operated over magnetic soil) [4].

AIB can be achieved with a number of different current source configurations. The simplest one is to use two separate current sources; one supplying the nominal excitation current to TX1 and the other supplying the same current with a superimposed compensation signal (shifted by 0˚ or 180˚) to TX2 .

The problem with this approach is that current sources of high accuracy (<1%) and resolution (<0.1%) are needed. The phase synchronization of their output signals might also become a challenging task.

The alternative current source configuration is shown in figure 7. With the proposed approach, the main current source is used for driving both TX1 and TX2 coils (I_m), while the secondary current source supplies only the small balancing current to TX2 coil (I_b). In this way, excitation and balancing functions are separated, which loosens the initial requirements on both current sources. The reference of the balancing source is fed from the current feedback circuit of the main source, so that I_m/I_b remains independent of I_m. For multi-frequency operation, this feature keeps the set balancing point constant for all components of the excitation current spectrum.

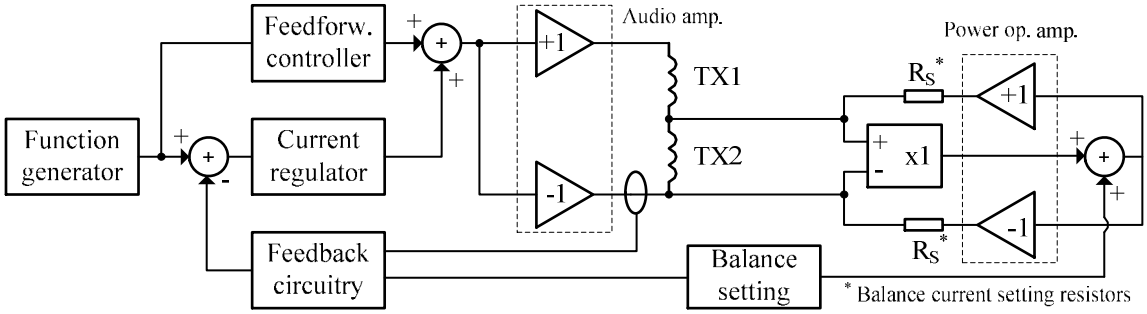

Figure 7. Block diagram of the proposed dual current source.

4. Results and discussion

Induction balance sensitivities to small perturbations of TX1 coil radius R_1, TX2 coil radius R_2 and RX coil radius r are calculated from equations (2.11), (2.12) and (2.13), respectively. For a selected sensing head geometry (R_1=15cm, R_2=6cm, r=4cm, N_1=12, N_2=4, N_r=180), the obtained sensitivities are $S_{R_1}^u$ = -1.057, $S_{R_2}^u$ = -1.555 and S_r^u = 0.498. The variations of the induced voltage imbalance Δu (in both relative and absolute terms) with respect to variations of R_1, R_2 and r (for three characteristic values of the respective parameter change) are given in table 1.

From the results given in table 1 it can be concluded that the IB sensitivities of the proposed coil configuration to ΔR_1, ΔR_2 and Δr are generally low. This can be also explained qualitatively, by observing the curves of spatial distribution of induced voltages corresponding to TX1 and TX2 coils near the sensor's centre, which are rather flat, figure 2. However, if combined effects from ΔR_1, ΔR_2 and Δr are taken into account and IB is observed in absolute terms, where N_r and ω bring a significant influence, the total sensor imbalance can become quite large, as shown in table 1.

In general, very careful coil design and high precision in the production of a sensing head are needed for practical application to landmine detection.

Table 1. Induction balance sensitivities to small variations of R_1, R_2 and r for a given sensor geometry.

TX1 coil radius		TX2 coil radius		RX coil radius		Induced voltage (excitation current, I=1A)		
							f=1kHz	f=100kHz
$\Delta R_1/R_1$ (%)	ΔR_1 (mm)	$\Delta R_2/R_2$ (%)	ΔR_2 (mm)	$\Delta r/r$ (%)	Δr (mm)	$\Delta u/u_{IB}$ (%)	Δu, (mV)	Δu, (V)
1	1.5	0	0.0	0	0.0	-1.057	3.1	0.310
2	3.0	0	0.0	0	0.0	-2.114	6.2	0.621
3	4.5	0	0.0	0	0.0	-3.171	9.3	0.931
0	0.0	1	0.6	0	0.0	-1.555	4.6	0.457
0	0.0	2	1.2	0	0.0	-3.110	9.1	0.913
0	0.0	3	1.8	0	0.0	-7.775	22.8	2.284
0	0.0	0	0.0	1	0.4	0.498	1.5	0.146
0	0.0	0	0.0	2	0.8	0.996	2.9	0.293
0	0.0	0	0.0	5	2.0	2.490	7.3	0.731

The dual current source, figure 7, and the analyzed sensing head configuration were implemented as laboratory prototypes, figure 8. The main current source is designed of the two bridge-mode audio amplifiers and the current feedback and control circuitry (I_n=1 A, f_H=100 kHz). The secondary current source is built from two power operational amplifiers with current control stage (I_n=100 mA). Laboratory function generator (Voltcraft VG-506) was used as a reference voltage source in the experiments. Voltage induced in RX coil, Δu, was fed to unity-gain instrumentation amplifier and measured with an oscilloscope. As a proof of AIB concept, Δu was measured at different frequencies (absolute value and normalized to u_{IB}) for a balanced sensor with passive IB (I_1=I_2) and with AIB, figure 9. The excitation current magnitude was set to 0.5A. Active balance was adjusted separately for each frequency. The results clearly indicate that the imbalances of the passive IB can be effectively compensated with AIB. Additional experiments are needed in order to fully characterise the method.

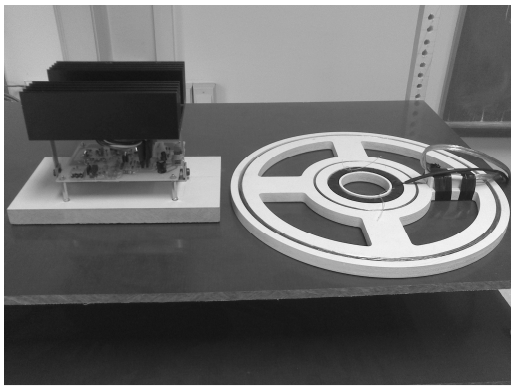

Figure 8. Implementation of laboratory prototypes (sensing head, current source).

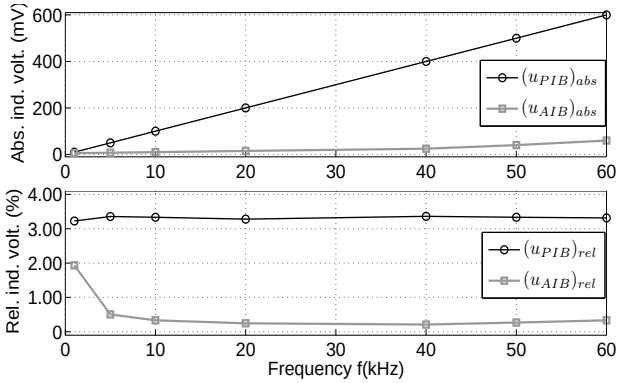

Figure 9. Magnitude of voltage induced in RX coil for passive IB and AIB at different frequencies.

5. Conclusions

For a design of novel, frequency-domain EMI landmine detector with additional model-based metal characterization features, we propose a sensing head configuration based on the transmitter-bucking approach. For this configuration, we analyzed the induction balance problem in terms of balance sensitivity to small perturbations of geometrical properties of the sensing head. The obtained results suggest that although the overall IB sensitivities are quite low, the total sensor imbalances expressed in absolute terms can become significant, therefore complicating the sensor design. In order to overcome this limitation and to explore new methods of coping with soil effects on IB, we developed and experimentally verified a prototype sensor with dual current source and active induction balance scheme. Future work will focus on further characterization of the method and new techniques for automatic compensation of imbalances caused by the effects of non-cooperative soils.

Acknowledgement

This work has been supported by the European Community Seventh Framework Programme under grant No. 285939 (ACROSS).

References

[1] Ishikawa J, Furuta K 2006 *Anti-personnel Landmine Detection for Humanitarian Demining* (London: Springer-Verlag London Limited)

[2] Bruschini C 2006 *A multidisciplinary Analysis of Frequency Domain Metal Detectors for Humanitarian Demining* (PhD Thesis:Vrije Universiteit Brussel)

[3] Won I J, Keiswetter D A, Hanson D R, Novikova E and Hall T M 1997 GEM-3 A Monostatic Broadband Electromagnetic Induction Sensor *J. Env. Eng. Geophys.* **2** 53-64

[4] Druyts P, Das Y, Craeye C, Acheroy M 2009 Modelling the Response of Electromagnetic Induction Sensors to Inhomogenous Magnetic Soils With Arbitrary Relief *IEEE Trans. Geosci. Rem. Sens.* **47** 8 2627-2638.